Chapter 2
Surface Forces Apparatus in Nanotribology

Carlos Drummond and Philippe Richetti

Abstract The Surface Forces Apparatus (*SFA*) has proven to be an excellent tool for research in nanotribology. It allows the study of single or multiple asperity contacts lubricated or not. The normal load, the contact area and the sliding velocity between the surfaces can be controlled and unambiguously measured with higher accuracy than in any conventional tribometer. Furthermore, an image of the surfaces in contact can be obtained as the surfaces are slid, allowing the monitoring of the real size and shape of the contact area and the distance or film thickness profile between the surfaces when atomically smooth surfaces are used. It is relatively simple to perform a comprehensive exploration of the full space of parameters to determine the important variables in the frictional behavior of the system. In this chapter the principles of operation and some experimental details of the Surface Forces Apparatus nanotribometer are described.

2.1 Introduction

The measurement of normal interaction forces between solids dates back to the 1920s, when Tomlinson investigated the interaction between crossed filaments of different metals [1]. Later, research groups in the Netherlands and Russia led by Overbeek and Derjaguin developed different techniques for measuring the force between surfaces of quartz or glass as a function of their separation [2, 3]. The example of these seminal pieces of work was promptly followed by many other groups. Particularly in Cambridge a remarkable body of work was accomplished, leading to the development of the Surface Forces Apparatus, *SFA*, by Tabor, Winterton and Israelachvili [4, 5].

The study of lateral forces between surfaces has a longer history. The problem of friction between surfaces attracted great thinkers as Da Vinci, Coulomb, Euler, Amontons and many others. A fascinating historical account of the history of

C. Drummond (✉) · P. Richetti
Centre de Recherche Paul Pascal, CNRS-Université Bordeaux 1,
Avenue Albert Schweitzer, 33600 Pessac, France
e-mail: drummond@crpp-bordeaux.cnrs.fr

P. Richetti
e-mail: richetti@crpp-bordeaux.cnrs.fr

E. Gnecco and E. Meyer (eds.), *Fundamentals of Friction and Wear on the Nanoscale*,
NanoScience and Technology, DOI 10.1007/978-3-319-10560-4_2

tribology was compiled by Dowson [6]. Friction has also been investigated with *SFAs* modified for that purpose; the first friction measurements using this technique date back to the 70's [7]. A decade later Briscoe and Evans reported extensive results on the study of friction of adsorbed monolayers in air [8]. Nevertheless, it was not until the late 80's that nanotribology studies with the *SFA* became a very active field of research. Since then, various modifications to the technique have been introduced. In the present chapter we describe the principles of operations and some experimental details of the SFA-nanotribometer.

2.2 Surface Forces Apparatus Technique: Generalities

In a typical *SFA*-nanotribometry experiment molecularly smooth mica surfaces are glued to cylindrically curved silica lenses, and used to confine thin films. The use of mica as a substrate for surface force experiments was originally proposed by Bailey and Courtney-Pratt [9]. The cylindrically-shaped silica disks are placed with their axes perpendicular to each other, a configuration that presents several advantages. First, it circumvents the difficult—if not impossible—task of accurately aligning two parallel plates. Unwanted edge effects are easily avoided by this approach. Second, it allows the investigation of different contact spots on the same pair of surfaces, simply by laterally displacing the crossed cylinders. If wear or contamination of the surfaces appears during the experiment, a fresh contact zone can be readily found. Finally, this geometry is convenient for comparing the results of the measurements with theoretical descriptions, typically sketched for flat surfaces. If the separation between the curved surfaces is much smaller than their radii of curvature, R, the *SFA* cross-cylinder configuration is equivalent to a sphere-on-plate contact. The force between two such surfaces, F, can be related to the energy of interaction between flat surfaces per unit area, E, by using the so-called Derjaguin approximation [10], $E = F/2\pi R$. This provides a normalization method in order to quantitatively compare data from different experiments. The question of the normalization of the measured interaction forces is more involved in friction experiments, as will be discussed below.

One of the major strengths of the *SFA* technique rests on the possibility of imaging the area of contact to determine the distance between the surfaces, the refractive index of the film confined between them and the geometry of the contact region. The *SFA* is one of few techniques in the field of tribology that allows to image in situ and in real time the geometry of the contact area, and probably the only one with subnanometric resolution. Multiple Beam Interferometry (*MBI*) is used for this purpose [11]. A highly reflective layer is deposited on the back side of the mica surfaces, and white light is passed through this built-in Fabry-Perot interferometer. The intensity of the light transmitted through the stratified media between the two mirrors depends on the optical thickness in a nontrivial way: only wavelengths that interfere constructively after the multiple reflections in the cavity traverse the multilayer system. The emerging beam of light can then be focused on a spectrometer. The resulting constructive interference fringes (Fringes of Equal Chromatic Order, *FECO*) carry with them the

information about the thickness and the refractive index of the different layers in the path of the light. Particularly, the thickness and the refractive index of the film confined between the mica surfaces can be determined with an accuracy of 0.1 nm and 0.01 respectively. Israelachvili developed simple explicit expressions to calculate these quantities from the wavelength of the *FECO* for a film confined between mica surfaces of identical thickness [12]. Later, the analysis has been extended to asymmetric, adsorbing, anisotropic or more complicated multilayer systems [13–15]. The potential of extending the analysis to obtain information about the roughness of the surfaces has also been demonstrated [16].

Many different experimental setups for the measurement of the surface forces have been reported. One of the oldest versions, the Mk I, was designed by Israelachvili and Adams for the measurement of forces between liquids and vapours [17]. It was based on the earlier designs of Tabor, Winterton and Israelachvili [4, 5], and was later followed by greatly improved and modified versions, the Mk II and III [18, 19]. Parker and co-workers developed later a circular steel apparatus (Mk IV) which is simpler to clean and assemble than Mk I or II [20]. The stability and reliability of the apparatus, as well as the simplicity of handling, have been progressively improved on each design. Recently, Israelachvili et al. have developed the SFA 2000, a device which is simpler to assemble and operate than earlier models and integrates a number of new functionalities [21]. The interested reader is referred to the original publications for the particular details of each apparatus.

For measuring the normal force of interaction in a typical *SFA* experiment, one of the surfaces is displaced using a combination of motors and piezoelectric elements, while the other surface is coupled to a calibrated spring with a fix end. Double cantilever springs are typically used in order to minimize the tilting and/or sliding between the surfaces when the spring is deflected. The interaction force between the surfaces is measured by progressively changing the distance between the fix end of the double cantilever spring and the second surface, and allowing the separation between the surfaces to come to an equilibrium situation where the surface forces are balanced by the elastic force of the spring. The difference between the displacement carried out and the actual change in the separation between the surfaces, Δx (measured by *MBI*) will correspond to a deflection of the spring. It will be used to calculate the difference in interaction force between the two equilibrium positions (before and after the motion), ΔF, by using Hooke's law, $\Delta F = k\Delta x$, where k is the elastic constant of the double cantilever spring. Albeit being conceptually simple, measuring the forces by this procedure is limited by spring instabilities. Quickly decaying forces, with a force-distance gradient larger than the spring constant are inaccessible because of the mechanical instability of the system under such conditions. Derjaguin et al. proposed the use of a force feedback technique to overcome this problem [3]. The idea is to control the force applied to the surfaces independently of the displacement: an external force is applied to the surfaces to maintain the spring undeflected. Effectively, this translates into a continuously changing spring constant, which eliminates the mechanical instability above mentioned. Several implementations of this idea have been reported [22–24]. Steward and Parker modified a Mark IV by incorporating a magnetic force transducer and a bimorph displacement sensor. Tonck et al. introduced

a feedback apparatus with capacitive displacement transducers [25]. An interesting description of the different techniques used for the measurement of the normal force between surfaces was presented by Lodge [26].

2.3 Surface Forces Apparatus Nanotribometer

In a nanotribology experiment with the *SFA*, the mica surfaces are brought to a certain separation, T. By using motors or electromechanical transducers a lateral displacement between the surfaces is imposed, and the force induced by this displacement is measured. Usually a certain normal load is applied, L. If the load is high enough, the glue layer under the surfaces undergoes elastic deformation, and a thin film is confined to a flat circular region of uniform thickness T and area of contact A, as illustrated in the Fig. 2.1. By using *MBI* an image of the surfaces in contact can be obtained as the surfaces are slid, allowing monitoring of the size and the profile of the contact area and the distance between the surfaces. Shear-induced elastohydrodynamic deformation can also be distinguished. In addition, damage of the surfaces can be easily detected as soon as it occurs, allowing to discriminate between undamaged sliding and friction with wear, and to independently study the two scenarios.

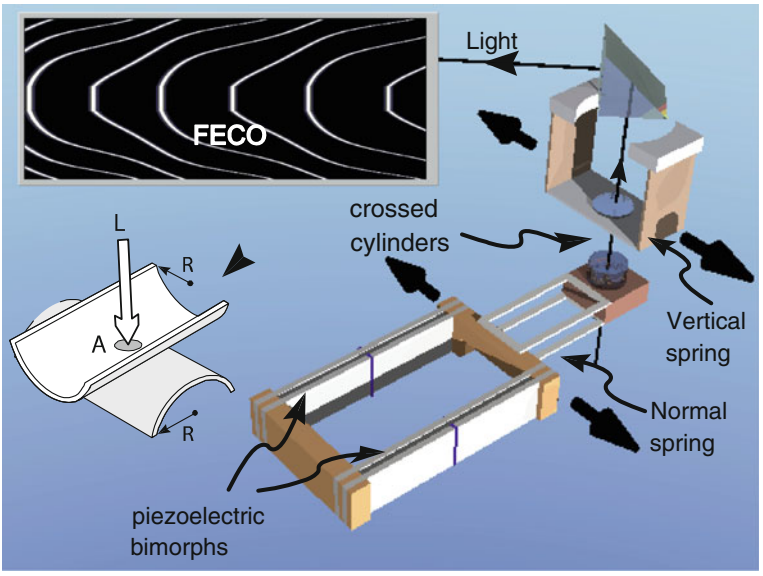

Fig. 2.1 Functional scheme of the *SFA* designed by Israelachvili et al. configured for friction experiments. The mica sheets are mounted in *crossed-cylinder* geometry, and their back surfaces are coated with reflective silver layers to allow for multiple beam interference. The *upper* and *lower* surfaces are mounted on cylindrically curved silica discs which are attached to the friction sensing device and the piezoelectric bimorph slider, respectively

A subject of major importance in the analysis of a *SFA*-nanotribology experiment is to identify the area over which the frictional force takes action. Often the friction force between sliding surfaces will be dominated by the flatten area. In that case, the sharp edge of the *FECO* allows recognizing the "area of contact", used to normalize the measured force and to calculate the shear stress. This operation is necessary to quantitatively compare the results of different experiments. From this point of view, the customary used friction coefficient is a less fundamental parameter than the shear stress. There is, however, an important caveat to this operation: very often the measured shear stress depends on the applied pressure. Given that curved surfaces are used in a *SFA* experiment, the normal pressure is not constant over the flatten area. Its value is given by a nonlinear function of the position in the contact area, a problem that has been extensively treated by the contact mechanics community [27]. It is clear then that the shear stress calculated in a *SFA* experiment is an average quantity, to be treated with caution.

An even more complicated scenario is found when there is a significant contribution to the friction force by regions of the surfaces outside the flatten area. This situation can be envisaged, for example, if there is a contribution to the friction coming from breaking and reforming bonds of long molecules that are able to bridge the two surfaces together. In that case, there is not an obvious way to identify the effective contact area. One possibility is to adopt a cut-off length, and to assume that the contribution to the frictional force is negligible at larger separations. However, at least two problems persist: the choice of the characteristic length rests somehow arbitrary and the contribution of a given region to the total force will most likely be a function of the local surface separation. It is important to emphasize at this point that the experimental difficulties just outlined are shared by most—if not all—the experimental techniques in nanotribology. Besides, the *SFA*-nanotribometer in its interferometric version is possibly the only technique in nanotribology that allows the observation of the contact geometry while rubbing the surfaces.

2.3.1 Experimental Setup

Several *SFA* experimental setups have been proposed during the last three decades, each with its own capabilities and limitations. In the following we will briefly describe few systems which are broadly used in the field. The reader interested in more complete information is referred to the original papers.

A number of experimental designs have been proposed by the group of Israelachvili [21, 28, 29]. The main features of the most recent version are illustrated in Fig. 2.1. The lower surface is mounted on a bimorph-driven slider [29], which moves laterally in a linear fashion when a constant slope voltage ramp is applied between the two electrodes of sectored piezoelectric bimorphs (electromechanical transducers). Alternatively, a constant frequency sinusoidal input can be imposed to the slider to perform nanorheological experiments. The upper surface is itself attached to a vertical double cantilever spring, whose deflection is monitored using strain gauges

connected to form the arms of a Wheatstone bridge. If the displacement of the lower surface induces a viscous or friction force on the upper surface, the vertical spring will deflect. From the deflection of this spring of known spring constant K, the friction force between the surfaces F can be calculated, simply by using Hooke's law of elasticity [28]. The mechanical properties of the measurement system (e.g., compliance and inertial mass) will influence the results; these factors have to be taken into account in order to obtain meaningful information from the signal measured. This can be done in a straightforward fashion in the *SFA* because of its mechanical simplicity and easy-to-characterize mechanical properties.

The maximal distance that can be slid with this setup depends on the characteristics of the bimorph strips used, being typically of the order of several tens of micrometers. A slider with a larger displacement range has been designed for the SFA 2000. A larger displacement can also be achieved by mechanically driving the upper surface using a reversible, variable speed motor-driver micrometer shaft that displaces the translation stage holding the vertical double cantilever spring. The detection limit for the friction force of this setup is typically of the order of several μN. By changing the frequency and the amplitude of the input signal to the bimorph slider, the driving speed can be typically varied between several Å/s to 0.1 mm/s. This device has been used to study a large number of systems. Some examples included confined simple liquids [30–32], polymer melt and solutions [28, 29, 33–35], self-assembled surfactant and polymer layers [36–38]. A number of systems in biotribology have also been extensively investigated [39, 40].

An alternative design conceived for the study of smaller deformations was introduced by Granick et al. [41, 42]. The goal of these low amplitude studies is to focus the investigation on the linear response of the confined films. By applying small deformations, the flow of fresh liquid in the contact zone is avoided. This allows the study of long time relaxation process that may be occurring in the contact region. A schematic of this device is illustrated in Fig. 2.2. In this design, the bottom surface remains stationary, while the upper surface is mounted on a holder attached to a double cantilever. Compared with the design of Israelachvili, they replaced the vertical metallic cantilevers by two piezoelectric bimorph strips. One of the bimorphs is used as an actuator and the other as a sensor. In the experiment, a voltage difference is applied to one of the bimorphs (actuator). Typically, a constant frequency sinusoidal signal is used, inducing an oscillating force on it. Simultaneously, the deformation-induced voltage of the second bimorph (sensor) is measured. This data is used to determine the actual displacement of the surface. By comparing this response with the one observed when no interaction between the two surfaces is presented, the influence of the confined film on the movement can be extracted. The electromechanical characteristics of the system are model as a series of effective masses, springs and dashpots representing the different components of the apparatus. The friction appears as a force acting on the holder of the lower surface, from which an effective viscosity can be extracted [42]. Although mainly conceived for the study of small deformations (of the order of the film thickness) typical displacements range from few nm to few

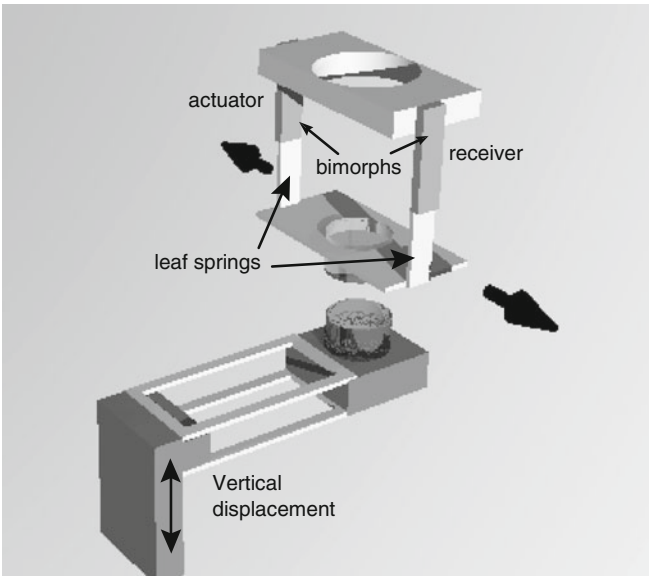

Fig. 2.2 Schematic illustration of the *SFA* designed by Granick et al. The shear force is generated by one bimorph (*actuator*) and the response of the device induces a voltage across the other bimorph (*receiver*)

μm. The reported sensitivity on the friction force is around 5 μN. Many different systems have been explored with this device, including simple liquids [41, 43–45] polymer melts [46–48] and solutions [49, 50].

A third experimental setup widely used in the literature has been developed by Klein et al. [51, 52]. A schematic of this device is presented in Fig. 2.3. In this device the sensitivity to the measured friction forces is greatly improved with respect to the previous designs. Inversely to the configuration adopted by Israelachvili et al. in the most recent version of their design the upper surface is driven and the effect on the lower surface is measured. A sectored piezoelectric tube is use to produce a normal or lateral displacement of the upper surface. An air-gap capacitor is used to measure the lateral displacement of the lower surface, which is coupled to a calibrated double cantilever spring with a fix end. The shear induced frictional force is then directly extracted from this displacement (e.g., the deflection of the spring) by using Hooke's law. The reported sensitivity of the friction force is 50 nN and the maximal displacement of the upper surface is few tens of μm. The improved sensitivity of this device comes from the detection method used. This has proven to be very valuable for the study of polymer melts and solutions [53–56] where small forces are typically observed. Research on water and other simple liquids has also been conducted with this experimental setup [57, 58]. Studies of several biotribological related systems have been recently reported [59, 60].

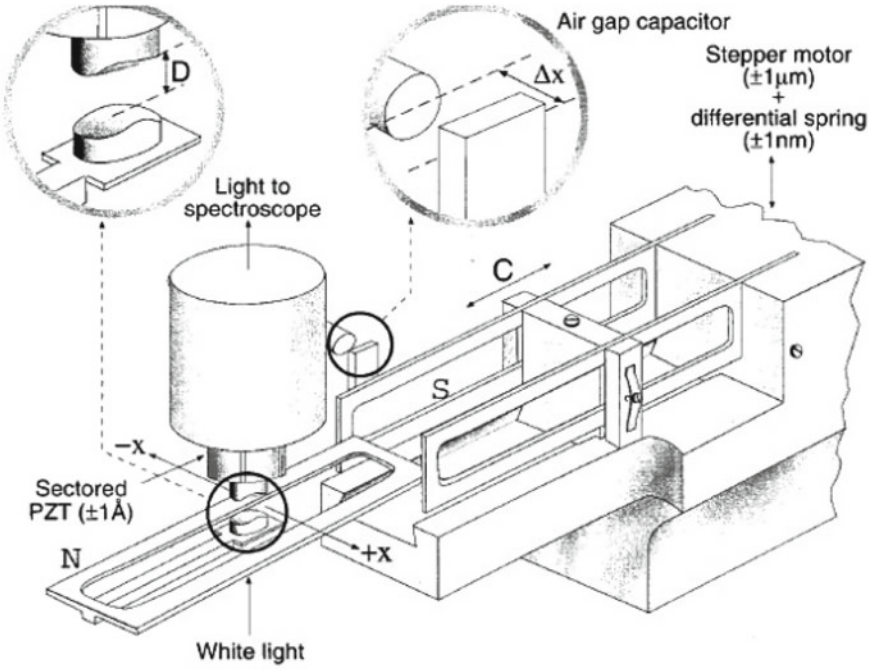

Fig. 2.3 Schematic illustration of the surface force balance (*SFB*) designed by Klein et al. The separation between the surfaces is controlled via a three-stage mechanism with a sectored piezoelectric tube on which the top surface is mounted. The piezoelectric element produces both normal and lateral displacement. The bending of the shear force spring is detected by an air-gap capacitor. Reprinted with permission from The *Journal of Physical Chemistry B* Volume **105(34)**, 8125–8134 (2001). Uri Raviv, Rafael Tadmor and Jacob Klein

As the SFA technique involves the displacement of curved surfaces, it is not a trivial matter to achieve large displacements under a constant applied load. In addition, achieving velocities greater than 100 μm/s can prove technically difficult and may involve large accelerations, due to the limited range of displacement. Bureau [61], and Israelachvili et al. [62] have addressed some of these issues. Qian et al. extended the capabilities of the apparatus to include the movement of the surfaces and the measurement of the friction force between them in two orthogonal directions in the plane of contact [63]. This new apparatus should prove to be useful in investigating shear-induced effects (e.g. shear alignment) on the confined thin films. Efforts in the same direction have also been pursued by Israelachvili et al. [21, 64].

Further improvements on different aspects of the experimental technique have been proposed during the last decade. First, substantial efforts have been devoted to automate the procedure of measurement, in order to improve the accuracy and simplicity of the technique. Second, the strategy used to determine the separation between the surfaces has been extended by using non-interferometric techniques. The automatic detection of the *FECO* have posed some challenges in the past, but increasingly

accurate and affordable charge couple devices in the market are currently used in several laboratories in the world for this purpose. Different strategies for the automation of the measurement process have been extensively described by Quon et al. [65], Grunewald and Helm [66], and more recently by Heuberger et al. [67].

As mentioned before, some efforts have also been devoted to determine the surface displacement by noninterferometric techniques. Several groups have proposed to use piezoelectric bimorphs for this purpose [68–70]. This solution is inadequate for long or quasi-static measurements due to the intrinsic drift and leakage of bimorph sensors (electrical drift and decay). A partial solution to these problems was presented by Parker [71], who suggested the use of an ultra-high impedance amplifier to lengthen the decay time of the bimorph sensor. A different method was presented by Frantz et al. [72]. They proposed to monitor the capacitance between the silver layers deposited on the back surface of the mica sheets for a fast detection of the surface separation, and described the use of this setup for the study of contact mechanics. Tonck et al. [25], and later Stewart [73], proposed to use capacitance dilatometry to measure the separation between the surfaces: one plate of a parallel-plate capacitor was attached to the moving surface, and the other to the chamber of the apparatus. This technique allows for a fast and accurate measurement of the displacement of the surface and eliminates the constraint of having to use transparent surfaces. A similar configuration, replacing one of the capacitors for a sensitive interferometric sensor to measure the deflection of the normal spring, has been used for very precise nanorheological studies [74]. Nevertheless, when opaque surfaces are used it is impossible to obtain an image of the contact region while shearing, which is one of the major strength of the SFA technique.

2.3.2 Local Structural Information: Combination of the SFA with Other Techniques

The information gathered in a conventional *SFA* experiment is limited to the average response of the confined film under shear. For achieving a better understanding of its behavior it is desirable to obtain structural information at the molecular level. Obtaining this information implies a colossal experimental challenge. On one hand the number of molecules involved in a thin film is relatively small, particularly when a localized area is explored, which inevitably reduces the intensity of any measured signal. On the other hand the investigated thin film is surrounded by layers of different materials that are susceptible to interact with the used probe (e.g. light, x-ray or neutrons) increasing the level of noise of the measured signal. Despite of these difficulties, several experimental groups have reported encouraging results of experiments combining the capabilities of the *SFA* with other techniques in-situ. It is reasonable to expect that techniques revealing the local molecular properties of the confined films will improve our understanding about the friction phenomena in the years to come.

The earliest effort in this direction aimed to combine *SFA* with x-ray diffraction (*XSFA*) [75, 76]. The second generation of *XSFA* combines the force measurement capabilities of the *SFA* with in-situ small angle x-ray scattering experiments [77]. Films of several liquid crystals have been studied with this technique, and the effect of shear on the molecular alignment in confined films has been directly evidenced. The application of this technique has so far been limited to films thicker than 500 nm, mainly because of the poor signal to noise ratio obtained otherwise. Obviously, the research in nanotribology calls for much thinner films. Moreover, the results reported with this method have been limited to an average investigation of the contact area, because of the size of the x-ray probe used. The possibility of investigating small regions of the contact area by using a micro focused x-ray beam has been suggested, but no results in this direction has been reported so far. Despite of the difficulties encountered, several research groups are actively working in this technique. It has been shown that X-ray reflectivity can be used to obtain structural information of ultra confined molecular films of OMCTS only few layers thick [78]. A recent publication describes an analogous study for water films [79]. Nevertheless, simultaneous determination of interaction forces and structural information in thin films has not been reported.

Helm et al. [80] showed that *MBI* can be used to obtain structural information of the confined thin films without any modification to the original *SFA* technique. Information about orientation and intermolecular interactions can be extracted from the *FECO* if optically active molecules are investigated. They were able to study ultra thin films, given that the light absorption by the confined molecules is enhanced by the multiple reflections in the optical cavity. Nevertheless, this technique limits the molecules that can be studied to large dye molecules. In addition, for best determination of the adsorption spectra of the confined dyes, relatively thick mica has to be used, reducing the accuracy of the film thickness determination.

In other order of ideas, Salmeron et al. suggested to couple second harmonic and sum-frequency generation to the *SFA* to study alignment and relaxation of confined ultra thin films, and showed the potential of the application by investigating self-assembled and Langmuir-Blodget monolayers of several surfactants [81]. However, results with other experimental systems have not been reported.

The combination of the *SFA* with other optical techniques has been limited by the reflective silver layer used to determine the surface separation by *MBI*. This layer strongly reduces the intensity of the illumination of the confined films, seriously limiting the in-situ performance of other optical methods. Granick et al. have overcome this limitation by replacing the reflective silver layer by multilayer dielectric coatings, which are transparent in different regions of the optical spectrum. In that way, they have been able to apply different spectroscopic tools to obtain in situ structural information of ultra thin films under shear [82, 83].

By combining the *SFA* nanotribometer with fluorescence correlation spectroscopy they measured the molecular diffusion coefficient in thin films within spots of submicron size, obtaining spatially resolved measurements [70]. This method has the drawback that fluorophore molecules have to be added to the liquid investigated in order to have a fluorescence signal. However, the authors have shown that the small

amount of fluorophores added didn't modify they behavior under shear and compression of the fluids investigated. Thus, diffusion coefficient of rhodamine in 1,2 propane diol was found to decrease by 2 orders of magnitude under confinement. Similar results were observed for the diffusion of cumarin 153 in OMCTS. They also found that the diffusion coefficient decreases from the edges towards the center of the contact region. Their results seem to suggest a heterogeneous dynamic in the confined thin films, where the diffusion appears to involve cooperative rearrangements of many molecules.

They have also reported results on the combination of *SFA* with Confocal Raman Spectroscopy [84]. The confocal geometry was used to reduced the bulk contribution to the measured signal. By using a multilayer reflective coating transparent to the argon laser and to the scattered Raman signal, they were able to monitor the geometry of the contact area simultaneously with the Raman scattering signal. They reported spatially resolved Raman scattering before and after shear, evidencing the influence of shear on the orientation of the molecules inside the confined film.

A third technique developed in Granick's group is the combination of photoluminescence and absorption dichroism with the *SFA* [85]. The shear-induced alignment of pre-adsorbed polymer molecules on mica was quantified both by photoluminescence and spectral absorption. They found molecular alignment parallel and perpendicular to the shear direction. which seems to be extremely sensitive to small changes in the initial conditions of the test. Although this technique is limited to the investigation of optical active substances, the information obtained can help to understand the behavior of lubricants with similar molecular structure.

In a different direction, Berg et al. recently suggested incorporating a Quartz Crystal Resonator in the *SFA* [86]. Because of the high oscillation frequency of the Quartz Crystal, this configuration allows the study of sliding velocities much higher than typically investigated in a conventional *SFA* nanotribology experiment. Nevertheless, in order to obtain meaningful results extremely thin mica surfaces need to be used, complicating its implementation as a routine technique. In addition, a sphere-on-plate geometry is required, which complicates the procedure of preparation of the mica surfaces.

2.3.3 Beyond Mica: Alternative Substrates

As mentioned previously, mica surfaces are the most popular substrates for *SFA* experiments. It gathers a set of properties seldom observed in other materials. It is transparent and can be prepared in the form of thin sheets of molecularly smooth surfaces over large areas by successive cleaving. The combination of these properties is at the heart of the *SFA* technique: transparent surfaces are required to determine the geometry of the contact by *MBI*. Besides, mica is a fairly incompressible material, so the forces measured are not flawed by the deformation of the surfaces. In addition it is inert to chemical reaction, so it is hardly modified during experiments. As a drawback, the process of producing mica surfaces thin enough to fulfill the requirements of the

SFA technique calls for a skillful experimentalist. This constraint is greatly relaxed by carefully implementation of automatic thickness measurement. On the other hand, thanks to the smoothness of the surfaces the geometry of the contact between the two surfaces can be easily described, simplifying the description and interpretation of the results.

The investigation of substrates other than mica is of interest for obvious reasons. The substrate plays a major role in most of the phenomena investigated by *SFA*, and particularly in tribology. It acts not only as a geometrical barrier, but as a major player: the interaction between the surfaces and with the confined films determines the general frictional behavior. For these reasons considerable efforts have been devoted to integrate different substrates in SFA experiments, to expand the range of applications of the technique. Mica surfaces can be modified by deposition or adsorption of different materials. By properly controlling the modification process, the smoothness of the surfaces can be preserved. In addition, modified surfaces may be more prone to chemical modifications.

Several groups have investigated the behavior of mica surfaces modified by self-assembly [37, 38, 87, 88] or deposition of Langmuir-blodgett films [37, 89, 90] of different substances. Mica acquires a negative surface charge when immersed in water, so positively charged species (e.g. cationic surfactants) spontaneously adsorbed on it; the structure of the adsorbed layer and its relationship to the molecular structure of the adsorbed material has been a very active area of research during the last 25 years [91]. The frictional behavior of the modified surfaces depends strongly on the characteristic of the adsorbed layers: surface properties like the adhesion energy and the morphology of the adsorbed layer will ultimately determine their behavior under shear.

As mentioned before, mica is an inert material. Nevertheless, it can be chemically modified by water vapor plasma treatment, increasing their reactivity to different species, e.g. chlorosilanes, as suggested by Parker et al. [92]. In this way, molecularly smooth hydrophobic surfaces can be prepared, given that the chemical structure is modified without increasing the roughness of the substrates. Mica surfaces treated by this procedure have been used in SFA studies [93]. Kessel and Granick modified this procedure to be able to induce the self-assembly of alkoxysilanes on mica, showing that strongly bound monolayers were formed [94].

Several groups have proposed to modify the mica surfaces simply by depositing on them thin films of different materials, including metals and dielectrics. In order to be able to monitor the geometry of the contact region by *MBI*, it is important for the deposited layers not to be completely opaque. This does not impose a serious limitation for sufficiently thin films. The interpretation of the *FECO* becomes more involved because of the larger number of optical layers in the optical path of the white light, but the information about the thickness and optical properties of the confined film can nonetheless be extracted. Different algorithms which are adequate for the modified experimental conditions have been described in the literature [95, 96].

Studies of mica modification by deposition of many different materials have been reported in the past. Silver [95, 97], gold [95, 98], platinum [98, 99], silica [99, 100], are only a few of a long list of materials investigated. Horn et al. grown single crystals

of aluminum oxide [101] by vapor phase condensation. The tribological behavior of these surfaces was later investigated by Berman et al. [102]. Vigil et al. deposited smooth layers of amorphous silica on mica, and study the behavior under compression and shear of the resulting surfaces [100]. They found that oscillatory structural forces were absent of the interaction between the surfaces due to the increased roughness. In addition, they observed long time-dependent adhesion and friction of the surfaces in the presence of water. Mc Guiggan et al. deposited amorphous carbon by magnetron sputtering on mica, and used these surfaces in the *SFA*-nanotribometer [103]. They found the friction force to be proportional to the area of contact between the surfaces, and the measured shear stress to decrease strongly with increasing relative humidity. Hirz et al. sputtered thin films of zirconia and alumina on mica, and investigated the behavior of these surfaces when lubricated with a linear perfluoropolyether [104]. They showed that these metal oxide formed smooth films on mica susceptible of being used as alternative substrates in *SFA* experiments.

Other groups have proposed to simplify the method of substrate preparation by eliminating the use of mica all together. A method of preparing silica surfaces for use in the *SFA* was proposed by Horn et al. although its use has not became widespread [105]. Golan et al. proposed to deposit a thin layer of silicon nitride on rigid silica disks previously coated with a reflective layer to replace the mica substrates [106]. They also reported a succinct tribological study of this generic substrate. Chain and Klein proposed to use mica as a template to produce extremely smooth gold surfaces [107, 108]. This method has been adapted by other groups to study electrochemical processes using the SFA [109, 110].

In general, the surface modification processes abovementioned may alter the smoothness of the surfaces at some degree complicating the geometry of the system, changing it from a single-asperity to a multiple-asperity contact. However, they allow the investigation of surfaces of interest in many different fields, extending the range of applications of the *SFA*. In addition, in most of the cases the roughness of the deposited layers can be controlled and/or modified to certain extent, allowing the investigation of the effect of surface roughness on friction, an important field of research on its own. *SFA* studies involving controlled roughness are in progress in several laboratories in the world [109].

2.4 Case Study: Weakly Adhesive Surfaces Under Shear

To illustrate the potential of the *SFA* technique for nanotribology studies, some experimental results obtained with self-assembled surfactant layers are described in this section.

We investigated the following system: the mica surfaces in the *SFA* are immersed in bulk aqueous surfactant solutions. Cationic surfactants are chosen, so that self assembled layers are formed on the mica surfaces. For surfactant concentrations above the critical micelle concentration (cmc) the adsorbed films show different morphology depending on the surfactant. Some surfactants adsorb as flat bilayers, while others

form rather modulated layers, suggesting the adsorption of globular or cylindrical micelles [91]. If two flat bilayers are compressed, eventually the hemifusion of the layers can be induced. In the hemifused region the mica surfaces end up cover by a monolayer of surfactant, and the surfaces are held together by an adhesive interaction, because of the hydrophobic attraction between the hydrophobic chains of the surfactant molecules. The precise measurement of the thickness of the trapped layer allows the clear identification of the hemifusion; an abrupt change of the confined film, corresponding to the expulsion of two monolayers from the contact region, is induced by compression and/or shear [38, 87, 111].

The behavior under shear of these systems is very complex. In general, when two intact bilayers are sheared, we do not detect any frictional resistance at any applied velocity or normal load: the friction force is below the detection limit of our experimental setup, which is similar to the one designed by Israelachvili [28, 29]. On the contrary, after the hemifusion of the layers is induced, a higher friction force can be observed. A typical friction trace measured during the hemifusion process is presented in Fig. 2.4, together with friction traces measured at different driving velocities after the hemifusion has taken place. The general behavior of the measured friction force with the driving velocity after hemifusion is illustrated in Fig. 2.5. At least 5 different regimes can be identified. At low velocities smooth sliding is observed. The force increases first linearly and then logarithmically with the driving velocity, before reaching a plateau. Above a certain critical velocity the movement becomes unstable and stick-slip is observed. At even higher velocities the movement becomes again stable and a second smooth sliding regime is observed, when the frictional resistance increases linearly with the driving velocity. As can be observed in the Fig. 2.5, an extensive dynamic regime is necessary to be able to observe the five regimes just described. This exploration of the space of parameters can be readily performed with the *SFA* nanotribometer.

Within the experimental accuracy, the shear stress, defined as $\sigma = F/A$, appears to be independent of the normal load L over the range of load investigated, both along the plateau regime preceding the stick-slip instability, and for the high velocity smooth-sliding regime. This implies that the friction force is proportional to the contact area A, rather than to the contact diameter or the load L. The load independence of the shear stress is no longer verified along the logarithmic regime. It is only due to the possibility of monitoring the real area of contact with the *SFA* (from the flat region on the *FECO*) that the shear stress can be univocally calculated at all times during the experiment.

All the trends observed in the sliding curve can be described by a model originally proposed by Schallamach [112] and that we have extensively discussed in the past [38]. The general behavior of the friction force can then be interpreted in terms of a model based on the kinetics of formation and rupture of small adhesive links (bonds) between the two shearing surfaces. Under this scenario, the observed stick-slip regime is just a manifestation of the mechanical instability due to the negative slope of the force versus velocity curve in a certain range of speeds. This adhesive model is insufficient to account for the steady smooth sliding regime observed at

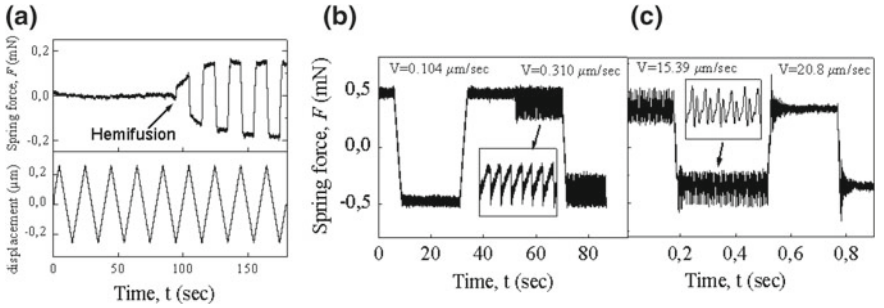

Fig. 2.4 **a** Friction signal recorded when the lower surface is displaced at constant velocity in a reciprocate mode, at the moment of the shear-induced hemifusion. A dramatic increase in friction force is accompanied by a film thickness reduction from 6.5 to 3.5 nm, indicating the hemifusion of the adsorbed bilayers. The normal load remains practically constant. **b** A smooth sliding regime is observed at low velocities, $V < V_c$. In the stick-slip regime the friction force oscillates between the kinetic value F_k and a *lower* kinetic value F_{sk}. **c** Increasing the driving velocity the measured spring force changes from an oscillatory state to a smooth steady state. Every time the driving velocity is reversed there is a transient response of few hundredth of a second before the system reaches steady-state sliding

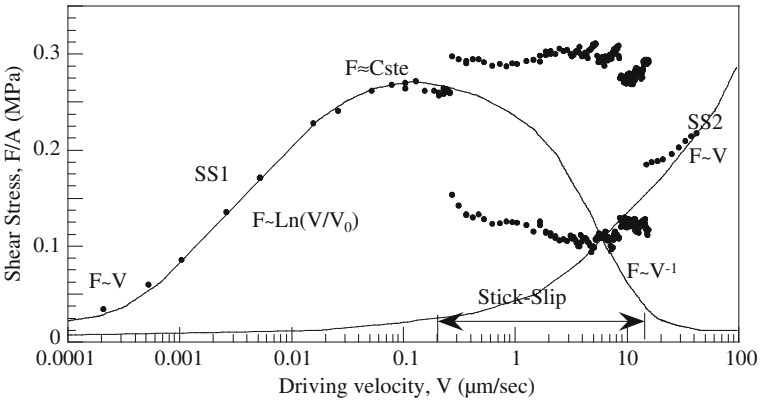

Fig. 2.5 Driving-velocity dependence of the shear stress measured while shearing two adsorbed monolayers of the 12-3-12-3-12 surfactant under a load of $L = 4.51$ mN at $T = 20$ C. The smooth sliding to stick-slip transition occurs at $V_c \approx 0.3$ μm/s. Prior to the transition, the kinetic stress σ_k levels off at V_1 after a logarithmic σ-V dependence. The quasi-smooth regime persists up to the transition at V_c. At high driving velocities a new transition to a smooth-sliding regime is observed

high velocities. A second contribution to the friction force (other than the elastic contribution) must be considered in order to re-stabilize the mechanical system in a kinetic state with finite friction. This extra contribution may be, for instance, the viscous dissipation in the trapped layer. The linear increase of the force at high sliding velocity seems to support this idea [38, 111].

This example illustrates the capabilities of the *SFA* nanotribometer. It shows how the measurement of the parameters pertinent to the friction problem, in particular the capability to monitor the geometry of the rubbing surfaces, greatly improves the understanding of the phenomena involved, allowing a quantitative comparison of the behavior of the system with theoretical models.

References

1. G.A. Tomlinson, Philos. Mag. **6**, 695–712 (1928)
2. J.T.G. Overbeek, M.J. Sparnaay, Discuss. Faraday Soc. **18**, 12 (1954)
3. Y.I. Rabinovich, B.V. Derjaguin, N.V. Churaev, Adv. Colloid Interface Sci. **16**, 63–78 (1982)
4. D. Tabor, R.H.S. Winterton, Proc. R. Soc. A **312**, 435–450 (1969)
5. J.N. Israelachvili, D. Tabor, Proc. R. Soc. A **331**, 19–38 (1972)
6. D. Dowson, *History of Tribology*, 2nd edn. (Professional Engineering Publishing Limited, London, 1998)
7. J.N. Israelachvili, D. Tabor, Wear **24**, 386–390 (1973)
8. B.J. Briscoe, D.C.B. Evans, Proc. R. Soc. A **380**, 389–407 (1982)
9. A.I. Bailey, J.S. Courtney-Pratt, Proc. R. Soc. A **227**, 500–515 (1955)
10. B. Derjaguin, Kolloid-Zeitschrift **69**, 155–164 (1934)
11. S. Tolansky, *Multiple Beam Interferometry of Surfaces and Films* (University Press, Oxford, 1948)
12. J.N. Israelachvili, J. Colloid Interface Sci. **44**, 259–272 (1973)
13. R.G. Horn, D.T. Smith, Appl. Opt. **30**, 59–65 (1991)
14. C. Mueller, P. Maechtle, C.A. Helm, J. Phys. Chem. **98**, 11119–11125 (1994)
15. M. Heuberger, Rev. Sci. Instrum. **72**, 1700–1707 (2001)
16. M. Heuberger, G. Luengo, J. Israelachvili, Langmuir **13**, 3839–3848 (1997)
17. J.N. Israelachvili, G.E. Adams, J. Chem. Soc., Faraday Trans. **1**(74), 975–1001 (1978)
18. J. Israelachvili, Proc. Natl. Acad. Sci. U. S. A. **84**, 4722–4724 (1987)
19. J.N. Israelachvili, P.M. McGuiggan, J. Mater. Res. **5**, 2223–2231 (1990)
20. J.L. Parker, H.K. Christenson, B.W. Ninham, Rev. Sci. Instrum. **60**, 3135–3138 (1989)
21. J. Israelachvili, Y. Min, M. Akbulut, A. Alig, G. Carver, W. Greene, K. Kristiansen, E. Meyer, N. Pesika, K. Rosenberg, H. Zeng, Rep. Prog. Phys. **73**, 036601 (2010)
22. J. Parker, A. Stewart, Prog. Colloid Polym. Sci. **88**, 162–168 (1992)
23. A.M. Stewart, J.L. Parker, Rev. Sci. Instrum. **63**, 5626 (1992)
24. W.H. Briscoe, R.G. Horn, Langmuir **18**, 3945–3956 (2002)
25. A. Tonck, J.M. Georges, J.L. Loubet, J. Colloid Interface Sci. **126**, 150–163 (1988)
26. K.G. Lodge, Adv. Colloid Interface Sci. **19**, 27–73 (1983)
27. K.L. Johnson, *Contact Mechanics* (Cambridge University Press, Cambridge, 1985)
28. A.M. Homola, J.N. Israelachvili, M.L. Gee, P.M. McGuiggan, J. Tribol. **111**, 675 (1989)
29. G. Luengo, F.-J. Schmitt, R. Hill, J. Israelachvili, Macromolecules **30**, 2482–2494 (1997)
30. M.L. Gee, P.M. McGuiggan, J.N. Israelachvili, A.M. Homola, J. Chem. Phys. **93**, 1895–1906 (1990)
31. J. Israelachvili, P. McGuiggan, M. Gee, A. Homola, M. Robbins, P. Thompson, J. Phys.: Condens. Matter **2**, SA89–SA98 (1990)
32. C. Drummond, J. Israelachvili, Phys. Rev. E **63**, 041506 (2001)
33. G. Luengo, J. Israelachvili, A. Dhinojwala, S. Granick, Wear **200**, 328–335 (1996)
34. P.A. Schorr, T.C.B. Kwan, S.M. Kilbey, E.S.G. Shaqfeh, M. Tirrell, Macromolecules **36**, 389–398 (2003)
35. G. Luengo, M. Heuberger, J. Israelachvili, J. Phys. Chem. B **104**, 7944–7950 (2000)
36. H. Yoshizawa, C. You-Lung, J. Israelachvili, Wear **168**, 161–166 (1993)

37. H. Yoshizawa, Y.L. Chen, J. Israelachvili, J. Phys. Chem. **97**, 4128–4140 (1993)
38. C. Drummond, J. Israelachvili, P. Richetti, Phys. Rev. E **67**, 066110 (2003)
39. B. Zappone, M. Ruths, G.W. Greene, G.D. Jay, J.N. Israelachvili, Biophys. J. **92**, 1693–708 (2007)
40. G.W. Greene, X. Banquy, D.W. Lee, D.D. Lowrey, J. Yu, J.N. Israelachvili, Proc. Natl. Acad. Sci. U. S. A. **108**, 5255–5259 (2011)
41. J. Van Alsten, S. Granick, Phys. Rev. Lett. **61**, 2570–2573 (1988)
42. J. Peachey, J. Van Alsten, S. Granick, Rev. Sci. Instrum. **62**, 463–473 (1991)
43. H. Hu, G. Carson, S. Granick, Phys. Rev. Lett. **66**, 2758–2761 (1991)
44. Y. Zhu, S. Granick, Phys. Rev. Lett. **87**, 096104 (2001)
45. A.L. Demirel, S. Granick, J. Chem. Phys. **115**, 1498 (2001)
46. S. Granick, H.-W. Hu, Langmuir **10**, 3857–3866 (1994)
47. S. Granick, H.-W. Hu, G.A. Carson, Langmuir **10**, 3867–3873 (1994)
48. J. Van Alsten, S. Granick, Macromolecules **23**, 4856–4862 (1990)
49. Y. Zhu, S. Granick, Macromolecules **36**, 973–976 (2003)
50. M. Ruths, S.A. Sukhishvili, S. Granick, J. Phys. Chem. B **105**, 6202–6210 (2001)
51. J. Klein, D. Perahia, S. Warburg, Nature **352**, 143–145 (1991)
52. U. Raviv, R. Tadmor, J. Klein, J. Phys. Chem. B **105**, 8125–8134 (2001)
53. R. Tadmor, J. Janik, J. Klein, Phys. Rev. Lett. **91**, 115503 (2003)
54. U. Raviv, S. Giasson, N. Kampf, J.-F. Gohy, R. Jérôme, J. Klein, Nature **425**, 163–165 (2003)
55. E. Eiser, J. Klein, T. Witten, L. Fetters, Phys. Rev. Lett. **82**, 5076–5079 (1999)
56. J. Klein, E. Kumacheva, D. Perahia, D. Mahalu, S. Warburg, Faraday Discuss. **98**, 173–188 (1994)
57. J. Klein, E. Kumacheva, J. Chem. Phys. **108**, 6996–7009 (1998)
58. U. Raviv, P. Laurat, J. Klein, Nature **413**, 51–54 (2001)
59. J. Seror, Y. Merkher, N. Kampf, L. Collinson, A.J. Day, A. Maroudas, J. Klein, Biomacromolecules **12**, 3432–3443 (2011)
60. J. Seror, Y. Merkher, N. Kampf, L. Collinson, A.J. Day, A. Maroudas, J. Klein, Biomacromolecules **13**, 3823–3832 (2012)
61. L. Bureau, Rev. Sci. Instrum. **78**, 065110 (2007)
62. D.D. Lowrey, K. Tasaka, J.H. Kindt, X. Banquy, N. Belman, Y. Min, N.S. Pesika, G. Mordukhovich, J.N. Israelachvili, Tribol. Lett. **42**, 117–127 (2011)
63. L. Qian, G. Luengo, D. Douillet, M. Charlot, X. Dollat, E. Perez, Rev. Sci. Instrum. **72**, 4171–4177 (2001)
64. E. Charrault, X. Banquy, K. Kristiansen, J. Israelachvili, S. Giasson, Tribol. Lett. **50**, 421–430 (2013)
65. R.A. Quon, J.M. Levins, T.K. Vanderlick, J. Colloid Interface Sci. **171**, 474–482 (1995)
66. T. Grünewald, C.A. Helm, Langmuir **12**, 3885–3890 (1996)
67. M. Zaüch, J. Vanicek, M. Heuberger, Rev. Sci. Instrum. **74**, 260–266 (2003)
68. J. Van Alsten, S. Granick, Tribol. Trans. **33**, 436–446 (1990)
69. J.N. Israelachvili, S.J. Kott, L.J. Fetters, J. Polym. Sci., Part B: Polym. Phys. **27**, 489–502 (1989)
70. A. Dhinojwala, S. Granick, J. Chem. Soc., Faraday Trans. **92**, 619 (1996)
71. J.L. Parker, Langmuir **8**, 551–556 (1992)
72. P. Frantz, N. Agrait, M. Salmeron, Langmuir **12**, 3289–3294 (1996)
73. A.M. Stewart, Meas. Sci. Technol. **11**, 298–304 (2000)
74. F. Restagno, J. Crassous, E. Charlaix, M. Monchanin, Meas. Sci. Technol. **12**, 16–22 (2001)
75. S. Idziak, I. Koltover, J. Israelachvili, C. Safinya, Phys. Rev. Lett. **76**, 1477–1480 (1996)
76. S.H. Idziak, C.R. Safinya, R.S. Hill, K.E. Kraiser, M. Ruths, H.E. Warriner, S. Steinberg, K.S. Liang, J.N. Israelachvili, Science **264**, 1915–1918 (1994)
77. Y. Golan, A. Martin-Herranz, Y. Li, C. Safinya, J. Israelachvili, Phys. Rev. Lett. **86**, 1263–1266 (2001)
78. O.H. Seeck, H. Kim, D.R. Lee, D. Shu, I.D. Kaendler, J.K. Basu, S.K. Sinha, Europhys. Lett. **60**, 376–382 (2002)

79. S. Chodankar, E. Perret, K. Nygård, O. Bunk, D.K. Satapathy, R.M. Espinosa Marzal, T.E. Balmer, M. Heuberger, J.F. van der Veen, Europhys. Lett. **99**, 26001 (2012)
80. P. Mächtle, C. Müller, C.A. Helm, J. Phys. II **4**, 481–500 (1994)
81. P. Frantz, F. Wolf, X.-D. Xiao, Y. Chen, S. Bosch, M. Salmeron, Rev. Sci. Instrum. **68**, 2499–2504 (1997)
82. A. Mukhopadhyay, J. Zhao, S.C. Bae, S. Granick, Rev. Sci. Instrum. **74**, 3067–3072 (2003)
83. S.C. Bae, J.S. Wong, M. Kim, S. Jiang, L. Hong, S. Granick, Philos. Trans. R. Soc., A **366**, 1443–154 (2008)
84. S.C. Bae, H. Lee, Z. Lin, S. Granick, Langmuir **21**, 5685–5688 (2005)
85. S.C. Bae, Z. Lin, S. Granick, Macromolecules **38**, 9275–9279 (2005)
86. S. Berg, M. Ruths, D. Johannsmann, Phys. Rev. E **65**, 026119 (2002)
87. P. Richetti, C. Drummond, J. Israelachvili, M. In, R. Zana, Europhys. Lett. **55**, 653–659 (2001)
88. M. Ruths, N.A. Alcantar, J.N. Israelachvili, J. Phys. Chem. B **107**, 11149–11157 (2003)
89. C.A. Helm, J.N. Israelachvili, P.M. McGuiggan, Biochemistry **31**, 1794–805 (1992)
90. S. Yamada, J. Israelachvili, J. Phys. Chem. B **102**, 234–244 (1998)
91. G.G. Warr, Curr. Opin. Colloid Interface Sci. **5**, 88–94 (2000)
92. J.L. Parker, D.L. Cho, P.M. Claesson, J. Phys. Chem. **93**, 6121–6125 (1989)
93. J.L. Parker, P.M. Claesson, D.L. Cho, A. Ahlberg, J. Tidblad, E. Blomberg, J. Colloid Interface Sci. **134**, 449–458 (1990)
94. C.R. Kessel, S. Granick, Langmuir **7**, 532–538 (1991)
95. J.M. Levins, T.K. Vanderlick, Langmuir **10**, 2389–2394 (1994)
96. M.T. Clarkson, J. Phys. D: Appl. Phys. **22**, 475–482 (1989)
97. J.L. Parker, H.K. Christenson, J. Chem. Phys. **88**, 8013–8014 (1988)
98. C.P. Smith, M. Maeda, L. Atanasoska, H.S. White, D.J. McClure, J. Phys. Chem. **92**, 199–205 (1988)
99. N.A. Alcantar, C. Park, J.-M. Pan, J.N. Israelachvili, Acta Mater. **51**, 31–47 (2003)
100. G. Vigil, Z. Xu, S. Steinberg, J. Israelachvili, J. Colloid Interface Sci. **165**, 367–385 (1994)
101. R.G. Horn, D.R. Clarke, M.T. Clarkson, J. Mater. Res. **3**, 413–416 (1988)
102. A. Berman, S. Steinberg, S. Campbell, A. Ulman, J. Israelachvili, Tribol. Lett. **4**, 43–48 (1998)
103. P.M. McGuiggan, S.M. Hsu, W. Fong, D. Bogy, C.S. Bhatia, J. Tribol. **124**, 239–244 (2002)
104. S.J. Hirz, A.M. Homola, G. Hadziioannou, C.W. Frank, Langmuir **8**, 328–333 (1992)
105. R.G. Horn, D.T. Smith, W. Haller, Chem. Phys. Lett. **162**, 404–408 (1989)
106. Y. Golan, N.A. Alcantar, T.L. Kuhl, J. Israelachvili, Langmuir **16**, 6955–6960 (2000)
107. L. Chai, J. Klein, Langmuir **23**, 7777–7783 (2007)
108. L. Chai, J. Klein, Langmuir **25**, 11533–11540 (2009)
109. M. Valtiner, X. Banquy, K. Kristiansen, G.W. Greene, J.N. Israelachvili, Langmuir **28**, 13080–13093 (2012)
110. T. Kamijo, M. Kasuya, M. Mizukami, K. Kurihara, Chem. Lett. **40**, 674–675 (2011)
111. C. Drummond, J. Elezgaray, P. Richetti, Europhys. Lett. **58**, 503–509 (2002)
112. A. Schallamach, Wear **17**, 301–312 (1971)